Cancer Cell
Article

Frequent Engagement of the Classical and Alternative NF-κB Pathways by Diverse Genetic Abnormalities in Multiple Myeloma

Christina M. Annunziata,[1,7] R. Eric Davis,[1,7] Yulia Demchenko,[2] William Bellamy,[5] Ana Gabrea,[2] Fenghuang Zhan,[5] Georg Lenz,[1] Ichiro Hanamura,[5] George Wright,[3] Wenming Xiao,[4] Sandeep Dave,[1] Elaine M. Hurt,[1] Bruce Tan,[1] Hong Zhao,[1] Owen Stephens,[5] Madhumita Santra,[5] David R. Williams,[5] Lenny Dang,[6] Bart Barlogie,[5] John D. Shaughnessy, Jr.,[5,7] W. Michael Kuehl,[2,7] and Louis M. Staudt[1,7,*]
[1] Metabolism Branch
[2] Genetics Branch
Center for Cancer Research, National Cancer Institute, Bethesda, MD 20892, USA
[3] Biometric Research Branch, Division of Cancer Treatment and Diagnosis, National Cancer Institute, Bethesda, MD 20892, USA
[4] Bioinformatics and Molecular Analysis Section, Computational Bioscience and Engineering Laboratory, Center for Information Technology, National Institutes of Health, Bethesda, MD 20892, USA
[5] Donna D. and Donald M. Lambert Laboratory of Myeloma Genetics, Myeloma Institute for Research and Therapy, University of Arkansas for Medical Sciences, Little Rock, AR 72205, USA
[6] Millennium Pharmaceuticals, Cambridge, MA 02139, USA
[7] These authors contributed equally to this work.
*Correspondence: lstaudt@mail.nih.gov
DOI 10.1016/j.ccr.2007.07.004

SUMMARY

Mechanisms of constitutive NF-κB signaling in multiple myeloma are unknown. An inhibitor of IκB kinase β (IKKβ) targeting the classical NF-κB pathway was lethal to many myeloma cell lines. Several cell lines had elevated expression of NIK due to genomic alterations or protein stabilization, while others had inactivating mutations of *TRAF3*; both kinds of abnormality triggered the classical and alternative NF-κB pathways. A majority of primary myeloma patient samples and cell lines had elevated NF-κB target gene expression, often associated with genetic or epigenetic alteration of *NIK*, *TRAF3*, *CYLD*, *BIRC2/BIRC3*, *CD40*, *NFKB1*, or *NFKB2*. These data demonstrate that addiction to the NF-κB pathway is frequent in myeloma and suggest that IKKβ inhibitors hold promise for the treatment of this disease.

INTRODUCTION

Multiple myeloma (MM), a malignancy of plasma cells (PCs), was diagnosed in over 16,000 people in the US in 2005 and contributed to over 11,000 deaths (Jemal et al., 2006). The current standard treatment of MM includes high-dose chemotherapy and stem cell transplantation. New agents with broad or undefined molecular specificity, such as the proteasome inhibitor bortezomib and the thalidomide analog lenalidomide (Barlogie et al., 2004; Mitsiades et al., 2004), can prolong survival but have associated toxicities. There is a clear need for new therapeutic strategies targeting defined pathogenetic events in MM.

Previous studies suggested the importance of NF-κB signaling in MM, by the nuclear presence of NF-κB in MM cells and the sensitivity of some MM cell lines to NF-κB inhibition (Hideshima et al., 2002; Hideshima et al., 2006). Within the bone marrow microenvironment, NF-κB signaling in stromal cells can lead to production of IL6, BAFF, or APRIL, known growth factors for and activators of NF-κB in MM (Hideshima et al., 2002; Marsters et al., 2000; Moreaux et al., 2005).

SIGNIFICANCE

Here we show the importance of classical NF-κB signaling in multiple myeloma. We discovered diverse genetic and epigenetic mechanisms leading to NF-κB activity in myeloma cell lines and patient samples. Targeted disruption of classical NF-κB signaling with a small-molecule inhibitor of IKKβ blocked myeloma cell proliferation and induced cell death. Most primary MM patient samples had evidence of NF-κB pathway activation, suggesting that therapeutic strategies targeting the classical NF-κB pathway should be pursued.

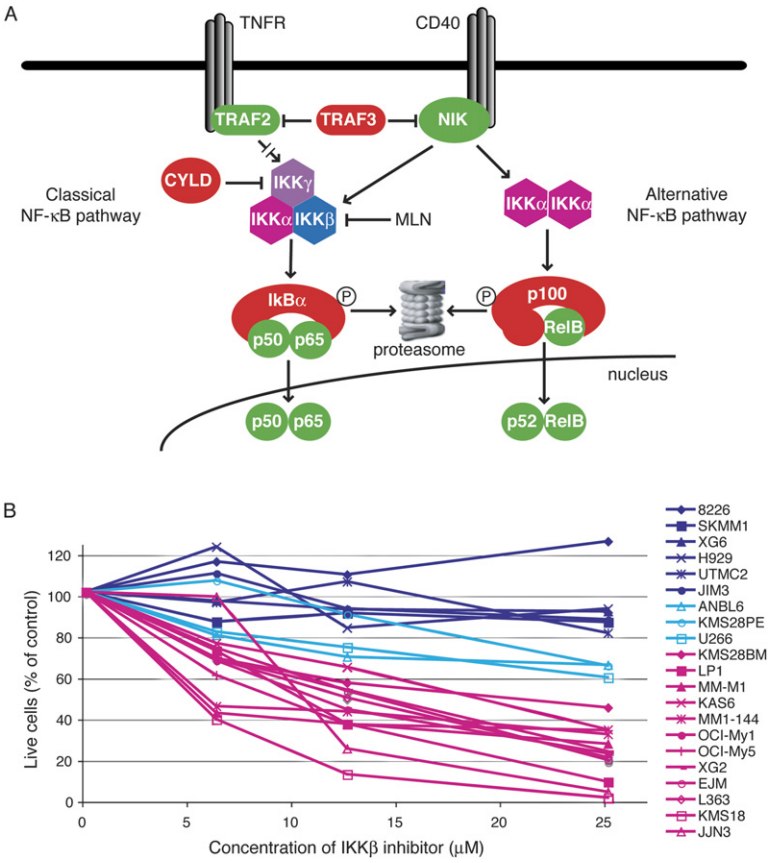

Figure 1. NF-κB Activation and IKKβ Inhibition

(A) Schematic of NF-κB signaling.

(B) Growth inhibition of MM cell lines by the IKKβ inhibitor MLN120b (MLN). Cell lines were cultured in the presence of MLN (25 μM), and cells were enumerated by flow cytometry as described (Davis et al., 2001). After 12 days, cell numbers were determined and displayed relative to a control culture treated with the same volume of DMSO (solvent) alone.

Five subunits combine into hetero- and homodimers to create the NF-κB transcription factor family (Ghosh and Karin, 2002), yielding two general pathways of activation (Figure 1A). In the classical pathway, IKKβ phosphorylates the inhibitory subunits IκBα, IκBβ, or IκBε, leading to their degradation in the proteasome. As a result, the NF-κB heterodimers p50/p65 and c-rel/p65 accumulate in the nucleus. In the alternative pathway, IKKα homodimers phosphorylate p100/NFKB2, resulting in proteasomal removal of an inhibitory C-terminal domain and generating the NF-κB p52 subunit (Senftleben et al., 2001; Xiao et al., 2001). Consequently, the p52/RelB heterodimers preferentially accumulate in the nucleus.

Various cancer types utilize constitutive NF-κB signaling to block apoptosis (Basseres and Baldwin, 2006), but the molecular mechanisms leading to constitutive IKKβ activation in cancer are largely unknown. Cancer-causing mutations in the NF-κB pathway could lead to overactivation of positive inputs to NF-κB activation, or loss of negative regulators. The NF-κB-inducing kinase (NIK) falls into the former category. NIK is necessary for alternative NF-κB signaling initiated by various members of the TNF receptor (TNFR) superfamily (Claudio et al., 2002; Coope et al., 2002; Ramakrishnan et al., 2004; Yin et al., 2001). However, NIK is required for signaling to the classical pathway by certain TNF family members, such as CD40 ligand and BAFF (Ramakrishnan et al., 2004). When overexpressed, NIK can activate the classical pathway, with resultant IκB degradation and nuclear translocation of p50/p65 and/or c-rel/p65 (O'Mahony et al., 2000; Woronicz et al., 1997).

Negative regulators act on many steps in the NF-κB pathway. TRAF3, a putative ubiquitin ligase, can inhibit signaling to both the classical and alternative NF-κB pathways by TNFR family members (Hauer et al., 2005) and may exert this effect, in part, by mediating NIK protein degradation (Liao et al., 2004; Xiao and Sun, 2000). The tumor suppressor CYLD inhibits the NF-κB pathway at multiple steps by deubiquitinating the IKKγ subunit, TRAF2, TRAF6, and BCL3 (Brummelkamp et al., 2003; Kovalenko et al., 2003; Massoumi et al., 2006; Regamey et al., 2003; Trompouki et al., 2003). The ubiquitin ligase cIAP1 can attenuate NF-κB signals via TNFR family members (Li et al., 2002; Rothe et al., 1995a).

In the present study, we discovered diverse genetic abnormalities causing constitutive NF-κB signaling in MM. Gene expression profiling revealed that the NF-κB pathway was activated in MM with surprising frequency. These genetic and functional data provide a molecular framework for the rational development of NF-κB pathway inhibitors for the therapy of multiple myeloma.

RESULTS

Sensitivity of Myeloma Cell Lines to IKKβ Inhibition

We examined the toxicity of a small-molecule inhibitor of IKKβ, MLN120b (MLN) (Nagashima et al., 2006), in 21 cell

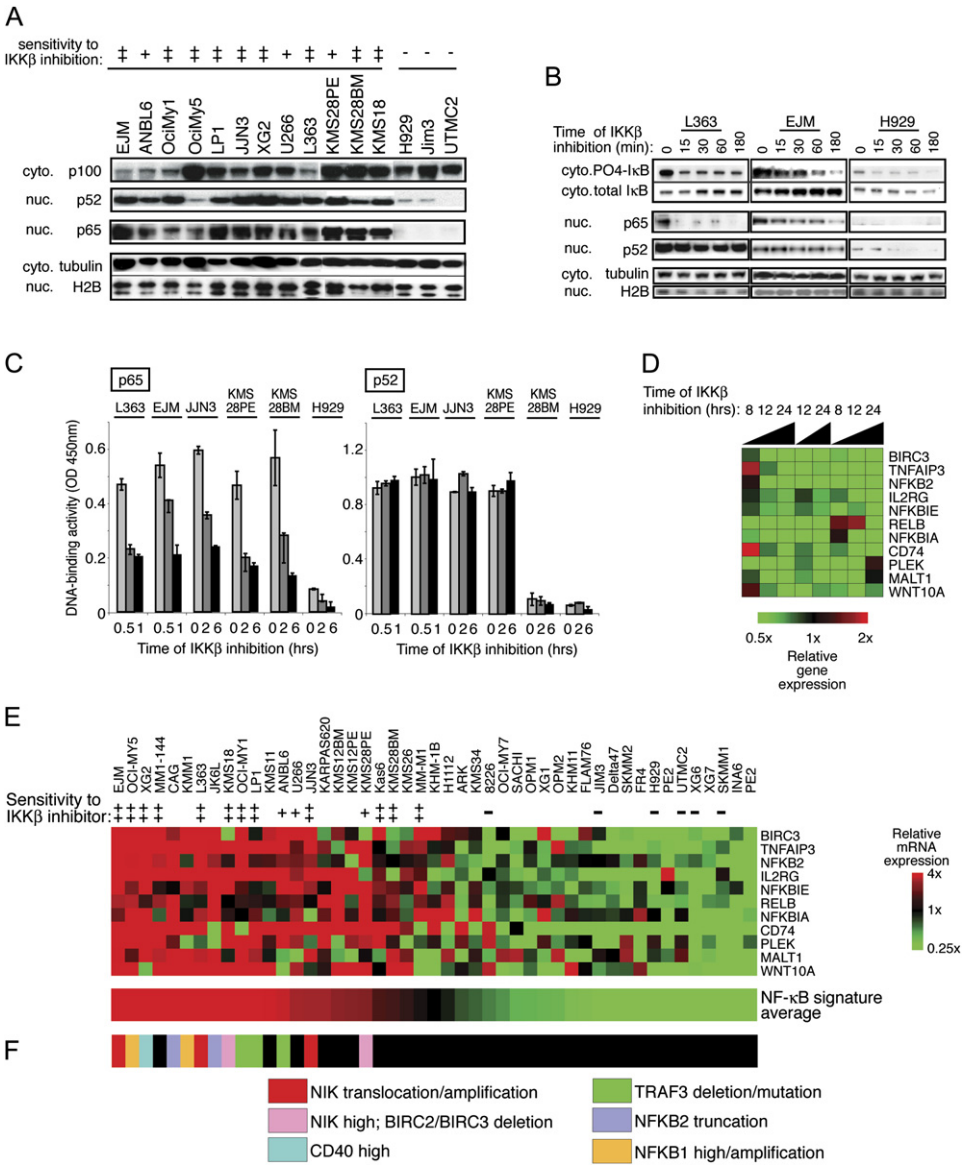

Figure 2. Effect of IKKβ Inhibition on NF-κB Signaling in MM Cells

(A) Steady-state levels of NF-κB subunits in cytoplasmic or nuclear-enriched protein fractions from cell lines.

(B) Effect of IKKβ inhibition by MLN on the abundance of NF-κB subunits and of total and phosphorylated IκBα.

(C) Effect of IKKβ inhibition on the nuclear DNA-binding activity of the NF-κB p65 and p52 subunits. Binding to an oligonucleotide containing the NF-κB consensus sequence was measured in nuclear extracts prepared from MM cells treated with MLN for the indicated times. DNA-binding activity was quantified by colorimetry (mean ± SD).

(D) NF-κB target genes in MM. L363 cells were treated with the IKKβ inhibitor MLN for the indicated times, and gene expression changes were assessed using DNA microarrays and depicted according to the color scale shown.

(E) Affymetrix U133plus2.0 microarray data from 47 MM cell lines were ordered using the average of the 11 NF-κB target genes determined in (D), median centered, and depicted according to the color scale shown.

(F) Abnormalities of NF-κB pathway components and regulators in the indicated cell lines.

lines representing many different molecular subgroups of MM. Twelve cell lines had moderate to high sensitivity, three had intermediate sensitivity, and six were resistant (Figure 1B). Cell lines showed varying degrees of apoptosis and growth arrest in response to IKKβ inhibition (Figure S1 in the Supplemental Data available with this article online).

The presence of nuclear NF-κB subunits in cell lines corresponded with their sensitivity to IKK inhibition. Nuclear p65 and p52 reflect activity of the classical and alternative NF-κB pathways, respectively. Both subunits were detected in nuclear extracts from 12 MLN-sensitive cell lines but were low or undetectable in nuclear extracts from three resistant lines (Figure 2A).

The level of IκBα phosphorylation decreased with IKKβ inhibition over time in two MLN-sensitive cell lines (Figure 2B). Nuclear p65 also decreased with MLN treatment, but nuclear p52 remained unchanged. NF-κB motif DNA-binding activity was measured in nuclear extracts from five sensitive cell lines and one resistant cell line. DNA binding by complexes containing p65 decreased after IKKβ inhibition, while p52 DNA binding was unaffected (Figure 2C). This result is consistent with the specificity of MLN for IKKβ and the classical NF-κB pathway (Nagashima et al., 2006).

We defined an NF-κB target gene signature by profiling gene expression changes with MLN treatment of L363 cells (Figure 2D). Eleven genes were consistently downregulated by IKKβ inhibition and correlated in expression across 47 cell lines (Figure 2E). These same genes were downregulated in MM cell line EJM upon retroviral expression of the IκBα super-repressor, a specific inhibitor of classical NF-κB signaling (Davis et al., 2001), which was toxic to both L363 and EJM cell lines (data not shown). The expression levels of these NF-κB target genes were combined to create an NF-κB signature average, which was used to rank the cell lines. Notably, all MLN-sensitive cell lines had higher NF-κB signature expression than the MLN-insensitive cell lines (Figure 2E).

NF-κB Activity and Genetic Abnormalities in Primary MM Cases

We analyzed the activity of the NF-κB pathway in gene expression profiles of 451 purified MM samples from newly diagnosed patients (Shaughnessy et al., 2007; Zhan et al., 2006). Each of the 11 NF-κB signature genes was significantly correlated in expression with the others in the primary MM samples (r value range 0.63–0.87; Figure 3A). Since these genes were identified solely based on activity of the NF-κB pathway in myeloma cell lines, their coregulation in primary patient samples suggests that they are surrogates for NF-κB pathway activity. Indeed, the proportion of MM cells with immunohistochemical evidence of nuclear p65 correlated with the NF-κB signature in patient samples ($r = 0.71$; $p < 0.001$) (Figure S2).

For each MM sample, the average of the 11 NF-κB signature genes was calculated and used to rank the samples (Figure 3A). Among the MM patient samples, 368 (82%) had levels greater than that of MM-M1, the NF-κB-dependent cell line with the lowest NF-κB signature expression. These data suggest that a majority of MM cases have functionally significant levels of the NF-κB signature, comparable to those in NF-κB-dependent cell lines.

We next compared the NF-κB signature levels in MM with those in normal PCs and in monoclonal gammopathy of undetermined significance (MGUS), a benign condition that can progress to MM. Normal PCs had levels of the NF-κB signature that were comparable, on average, to those in MGUS and MM (Figure 3C). Among normal human B cell subpopulations, PCs had the highest expression of the NF-κB signature (Figure 3D), consistent with their dependence on signals in the bone marrow microenvironment that trigger NF-κB (O'Connor et al., 2004). The high expression of the NF-κB signature in many MM cases may therefore reflect a similar dependence on the microenvironment. However, not all molecular subgroups of MM had equivalent expression of the NF-κB signature: the MF and LB subgroups had relatively high expression, while a proliferative (PR) subgroup had low expression (Figure 3E). Thus, the importance of the NF-κB pathway may be contingent upon other molecular features of these MM subgroups (Shaughnessy et al., 2007 Zhan et al., 2006).

To search for oncogenic abnormalities that might confer cell-autonomous NF-κB pathway activation in MM, we evaluated the expression of known regulators of NF-κB in patient samples. Genes with an "outlier" expression profile are those with a dramatically high or low expression in a subset of samples, which might reflect oncogenic events such as translocations, amplifications, or genomic deletions. Recently, a method to identify outlier genes was described, which relies on a scaling transformation of the expression data to accentuate extreme values (Tomlins et al., 2005). A similar method identified MM cases with FGFR3 and Cyclin D1 translocations (Zhan et al., 2002). We modified this approach to account for gene expression differences between known MM subgroups, attempting to focus on outliers associated with NF-κB activation in several MM subgroups (see Experimental Procedures). We chose a high cutoff for outlier gene expression to focus on cases most likely to have genetic abnormalities affecting mRNA expression levels.

Four candidate NF-κB regulators—*NIK*, *CD40*, *TRAF3*, and *CYLD*—had outlier mRNA expression values in at least five MM cases. For *NIK* and *CD40*, outlier cases highly overexpressed the corresponding mRNA, whereas for *TRAF3* and *CYLD*, outlier cases had exceedingly low mRNA levels (Figure 3F). In addition, six cases with high NF-κB signature expression had exceedingly low expression of *BIRC3* and the neighboring gene *BIRC2*, which was notable since *BIRC3* is in the NF-κB signature. Cases with outlier levels of these NF-κB regulators were significantly skewed toward high NF-κB signature expression (Figure 3B). In many cases, the altered expression of the outlier genes was due to genetic abnormalities (see below).

Aberrations of the NIK Genomic Locus in MM

We first investigated the molecular basis for outlier expression of *NIK*, a kinase capable of activating both the alternative and classical NF-κB pathways (Claudio et al., 2002; Coope et al., 2002; O'Mahony et al., 2000; Ramakrishnan et al., 2004; Woronicz et al., 1997; Yin et al., 2001). Five patient samples were clear outliers, with average expression that was 8.8-fold above the median (Figures 3B and 3F; Figure S3). *NIK* outliers had high expression of the NF-κB signature (Figures 3B and 3G).

By fluorescence in situ hybridization (FISH), three *NIK* outlier cases had chromosomal translocations between the *NIK* locus and the *IGH* locus (two cases) or the *IGL* locus (one case) (Figure 4A). Since chromosomal translocations or high-level amplifications lead to monoallelic

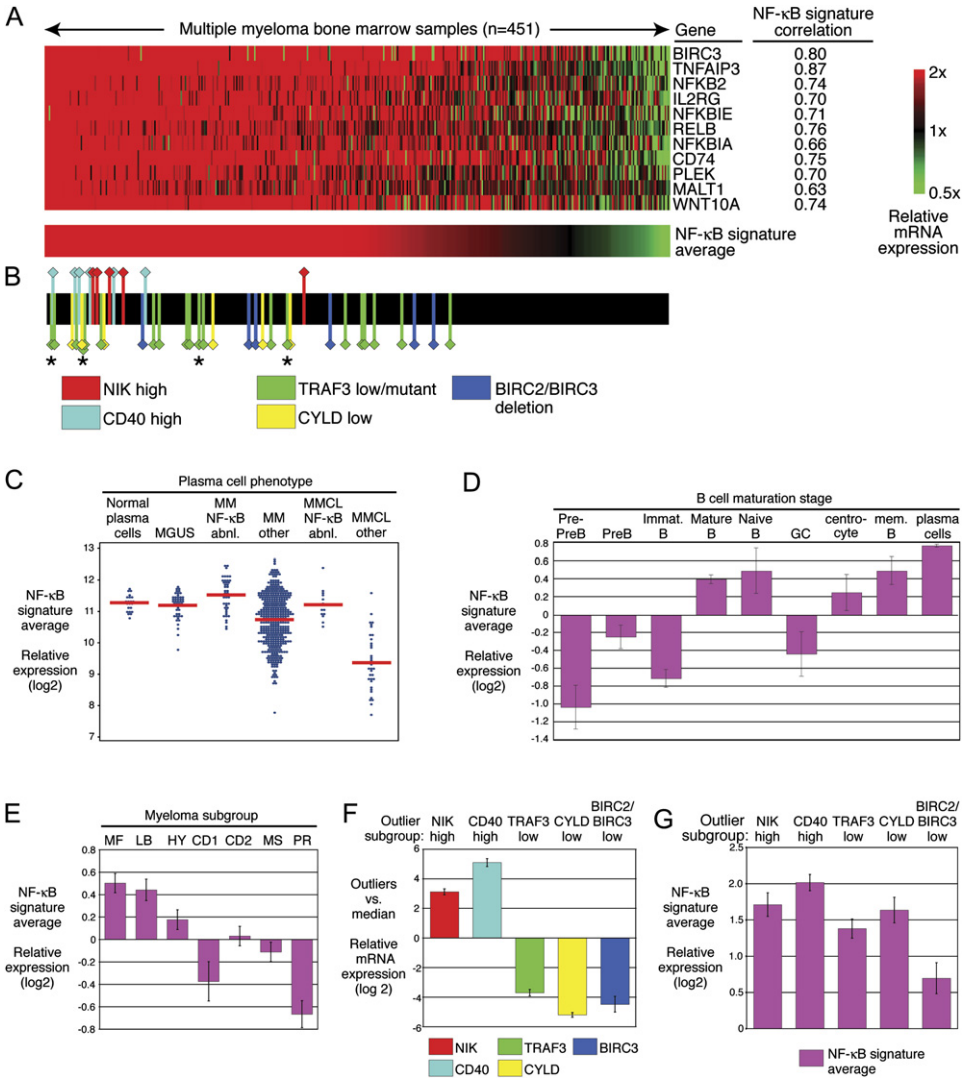

Figure 3. Multiple Molecular Mechanisms Activate NF-κB in Bone Marrow PC from Untreated MM Patients

(A) Expression of NF-κB target genes in primary MM patient samples. Affymetrix U133plus2.0 gene expression profiling data from 451 purified bone marrow plasma cell populations derived from untreated patients with MM (Zhan et al., 2006). Samples are ranked according to the average expression of the 11 NF-κB target genes. Expression was centered based on the median value in the MM cell lines (Figure 2E).

(B) MM samples with outlier gene expression and/or *TRAF3* mutations. Cases with high *NIK* or *CD40* expression and cases with low *TRAF3*, *CYLD*, or *BIRC2*/*BIRC3* expression are indicated with colored markers. The remaining cases are indicated in black. The asterisks indicate cases with inactivating TRAF3 mutations.

(C) NF-κB signature expression in normal and malignant plasma cell types. Data are taken from Zhan et al. (2006, 2007).

(D) NF-κB signature expression at different stages of human B cell differentiation. Duplicate samples from each stage were profiled.

(E) Expression of the NF-κB signature in MM gene expression subgroups.

(F) Expression of the indicated genes in the cases with outlier expression versus other MM cases.

(G) Expression of the NF-κB signature in outliers. Shown is the NF-κB signature expression in outliers relative to the minimum expression in MM cell lines sensitive to IKKβ inhibition.

In (D)–(G), the mean value ± SE is depicted.

mRNA expression, we developed RT-PCR assays to distinguish two common *NIK* alleles that differ by a single nucleotide polymorphism (SNP). Three *NIK* outlier cases had monoallelic *NIK* mRNA expression, one of which was confirmed to have a translocation of *NIK* by FISH (Figure 4A). Among four cases with intermediate (but not outlier) *NIK* expression, *NIK* mRNA was expressed from both alleles, consistent with transcriptional overexpression (Figure 4A).

Two NF-κB-dependent cell lines (EJM, L363) had *NIK* mRNA levels equivalent to those in the *NIK* outlier patient samples (data not shown). In the EJM cell line, the *NIK*

A

Patient	NIK expression category	NIK expression (Fold > median)	Trans-location	Allelic expression
1	outlier	13.45	NIK-Igλ	nd
2	outlier	12.56	nd	one
3	outlier	12.54	nd	one
4	outlier	11.47	NIK-IgH	nd
5	outlier	6.68	NIK-IgH	one
6	intermediate	3.44	nd	both
7	intermediate	2.85	nd	both
8	intermediate	2.75	nd	both
9	intermediate	2.50	nd	both

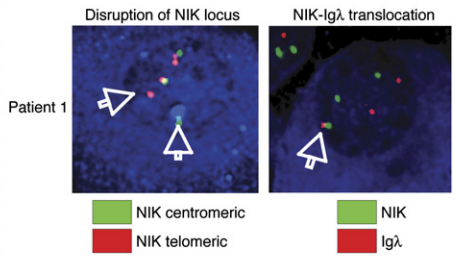

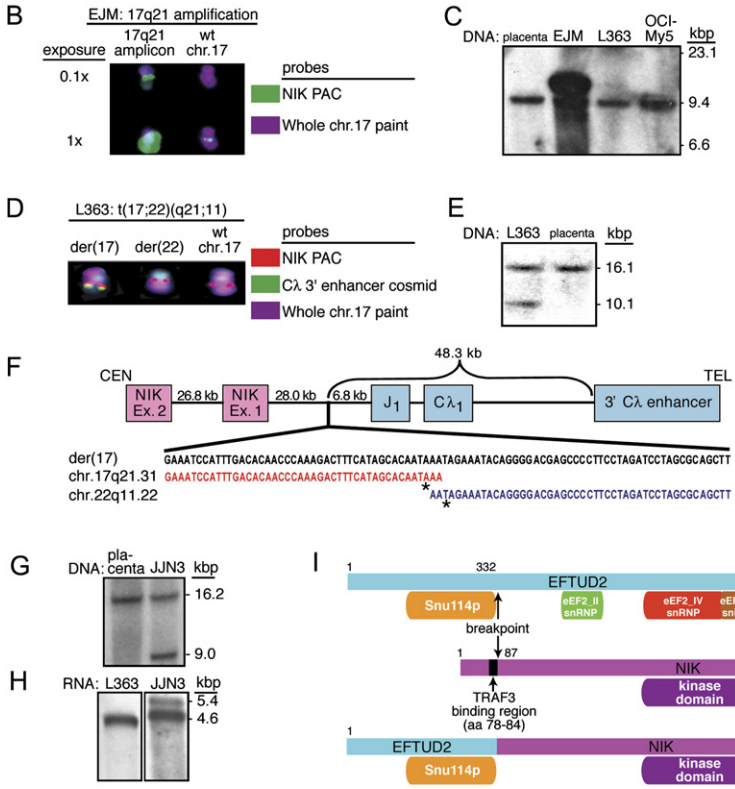

Figure 4. Amplification or Translocation of NIK in MM Cell Lines

(A) Chromosomal translocations of NIK in primary MM patient samples. Three samples with *NIK* translocated to either the *IGH* locus or the *IGL* locus were documented by FISH (one representative sample shown at right). Other cases had monoallelic expression of *NIK*, consistent with a chromosomal translocation or other *cis*-acting event (see text for details). nd, not done.

(B) FISH analysis of *NIK* amplification in the EJM cell line. Two exposures are shown to illustrate the high-level *NIK* amplicon on 17q21.

(C) Southern blot of *NIK* amplification in the EJM cell line. Genomic DNAs from the indicated cell lines were digested with HindIII and hybridized with a radiolabeled 568 bp PCR fragment amplified from *NIK* exon 15.

(D) FISH analysis of *NIK* translocation to the *IGL* locus in the L363 cell line. The signal from the 92 kb *NIK* PAC probe is split between the der(17) and der(22) chromosomes and is also present on the wild-type chr 17. The der(17) contains *NIK* sequences juxtaposed to the *IGL* enhancer.

(E) Southern blot of the *NIK* translocation in the L363 cell line. HpaI digest of genomic DNA hybridized with a *NIK* probe (Chr17:40,769,557-40,770,000 [build35]) shows a 16.1 kb wild-type fragment in placental DNA and a 10.1 kb fragment in L363.

(F) Structure of the *NIK* translocation breakpoint in L363. CEN, centromeric end; TEL, telomeric end. The breakpoint on chr 17 is bp 40,778,164 (asterisk) and on chr 22 is bp 21,553,824 (asterisk) (NCBI build 35).

(G) Southern blot of the *NIK* translocation in JJN3 cells. HpaI digest of genomic DNA hybridized with *NIK* exon 5 probe shows the wild-type locus as a 16.2 kb fragment. The translocated locus is a 9.0 kb fragment.

(H) Northern blot of *NIK* mRNA species. mRNA from L363 or JJN3 cells was hybridized with a radiolabeled cDNA probe derived from the 3′ end of the *NIK* mRNA. A wild-type 4.6 kb mRNA species was detected in L363 cells (17 hr exposure). JJN3 cells (5 day exposure) show the wild-type mRNA and an additional 5.4 kb mRNA, presumably from the translocated allele.

(I) Schematic of the EFTUD2-NIK fusion protein in JJN3 (see text for details).

locus was highly amplified, as judged by both FISH and Southern blot (Figures 4B and 4C). In the L363 cell line, FISH revealed a chromosomal translocation juxtaposing the *NIK* and the *IGL* locus (Figures 4D and 4E). The breakpoint occurred 28 kb 5′ of *NIK*, bringing the *NIK* promoter in proximity to *IGL* enhancer elements (Figure 4F).

In the JJN3 cell line, one *NIK* allele generated an aberrant restriction fragment that hybridized with a probe derived from *NIK* exon 5 (Figure 4G). These cells expressed a 5.4 kb *NIK* mRNA instead of the wild-type 4.6 kb species (Figure 4H). Cloning of the aberrant *NIK* allele identified a translocation fusing a 5′ fragment of *EFTUD2* to a 3′ portion of *NIK*, with the breakpoint between exons 11 and 12 of *EFTUD2* and between exons 2 and 3 of *NIK* (Figure S4). The translocation is predicted to generate a 5152 bp mRNA encoding a 132 kD in-frame EFTUD2-NIK fusion protein (Figures 4H and 4I), and these cells indeed expressed an aberrant, high-molecular-weight NIK protein (Figure 6A). The EFTUD2-NIK fusion protein consists of the N-terminal region of EFTUD2, containing a conserved domain of unknown function, fused to the C-terminal NIK kinase domain (Figure 4I).

Mutations, Deletions, and Silencing of TRAF3 in MM

By the outlier approach, 17 MM cases had low expression of *TRAF3*, a negative regulator of NIK (Liao et al., 2004; Xiao and Sun, 2000). On average, outliers expressed *TRAF3* mRNA at levels 13-fold below the median (Figures 3B and 3F; Figure S3). *TRAF3* outliers had high expression of the NF-κB signature (Figures 3B and 3G).

In the NF-κB-dependent cell line OCI-My1, which does not express *TRAF3* mRNA, the *TRAF3* gene could not be amplified by PCR from genomic DNA (data not shown), and array-based comparative genomic hybridization (aCGH) analysis confirmed a homozygous *TRAF3* deletion (Figure 5A). We next constructed a quantitative PCR (qPCR) assay for *TRAF3* genomic copy number. Of the six *TRAF3* outliers analyzed, two had biallelic deletion, three had monoallelic *TRAF3* deletion (one of which had a *TRAF3* mutation on the remaining allele), and one had a normal copy number (Figure 5B). In these cases, epigenetic silencing or decreased mRNA stability due to nonsense mediated decay may contribute to the low *TRAF3* mRNA expression; indeed, case P993 had a frameshift mutation of TRAF3 that resulted in early termination of the protein (see below). Homozygous deletions of *TRAF3* were not present in other "NF-κB-high" cases (NF-κB signature above the median; n = 12) or in NF-κB-low cases (NF-κB signature in the lowest quintile; n = 12).

Next, we investigated whether somatic mutations might inactivate TRAF3 in MM. We sequenced 11 exons of *TRAF3* in genomic DNA from ten cell lines and 47 samples from newly diagnosed MM patients, including 6 *TRAF3* outliers, 29 NF-κB-high cases, and 12 NF-κB-low cases. Two cell lines and four patient samples had mutations resulting in stop codons in exons 4, 9, 10, or 11 (Figure 5C). All of these had high NF-κB signature expression (Figures 2F and 3B). The predicted TRAF3 protein in the LP1 cell line would lack the C-terminal 283 amino acids, containing the entire MATH domain crucial for interaction of TRAF3 with NIK and with members of the TNFR superfamily (Li et al., 2003; Liao et al., 2004; Ni et al., 2000, 2004). Likewise, mutations in patient samples 727, 993 and 1645 would remove the entire MATH domain. In the ANBL6 cell line, the C-terminal 144 amino acids would be lost due to the mutation, producing a protein in which the MATH domain is disrupted. The mutation in patient sample 83 would similarly truncate the protein within the MATH domain. Of note, all *TRAF3* mutations were homozygous, suggesting a strong selective pressure for these mutations in MM.

CYLD Deletion in NF-κB-Positive MM

Among genes that were silenced in outlier cases, the NF-κB regulator most significantly associated with high NF-κB signature expression was *CYLD*, a known negative regulator of NF-κB signaling (Brummelkamp et al., 2003; Kovalenko et al., 2003; Regamey et al., 2003; Trompouki et al., 2003). Six MM cases had expression of *CYLD* mRNA that was, on average, 37-fold below the median (Figures 3B and 3F; Figure S3). CYLD outliers had high expression of the NF-κB signature (Figures 3B and 3G).

We quantified *CYLD* copy number by qPCR in five available samples from *CYLD* outliers and found biallelic loss of the locus in all (Figure 5E). Analysis of published aCGH data from some of these cases (Carrasco et al., 2006) confirmed that the sixth *CYLD* outlier also had a biallelic *CYLD* deletion (Figure 5D). In summary, homozygous *CYLD* deletions were present in all *CYLD* outliers and are thus a recurrent genetic event in multiple MM that is associated with high NF-κB activity.

CD40 Overexpression in MM

CD40 signaling activates both the classical and alternative NF-κB pathways (Berberich et al., 1994; Coope et al., 2002; Qing et al., 2005; Ramakrishnan et al., 2004). Six outlier cases expressed *CD40* mRNA levels that were 34-fold above the median (Figures 3B and 3F; Figure S3). *CD40* outliers had high expression of the NF-κB signature (Figures 3B and 3G). Of note, the NF-κB-dependent cell line XG2 expressed *CD40* mRNA at a 24-fold higher level than the average in other cell lines, suggesting that it may have originated from a *CD40* outlier MM case. Since CD40 is an NF-κB target gene in certain lymphoma types (Lam et al., 2005), we investigated whether the high *CD40* expression in the outliers could be due to their high NF-κB signature expression. We chose 60 control cases with an average NF-κB signature expression equivalent to that of the outliers. In these controls, the average *CD40* expression was 23-fold lower than that of the outliers ($p = 5.2 \times 10^{-9}$). Therefore, the high *CD40* expression in the outliers is not primarily due to their NF-κB activity.

qPCR of the *CD40* locus in three of the outlier cases did not reveal high-level amplification, nor did the XG2 cell line have *CD40* amplification by aCGH (data not shown). The mechanism of *CD40* overexpression in these cases is currently unknown but could be due to chromosomal translocation or *trans*-acting regulatory mechanisms.

Other Genetic Abnormalities Affecting the NF-κB Pathway in MM

Several cell lines had high NF-κB signature expression but lacked genetic alterations in *NIK*, *TRAF3*, *CD40*, or *CYLD* (Figure 2F). We therefore examined these cell lines for alterations in other components of the NF-κB pathway.

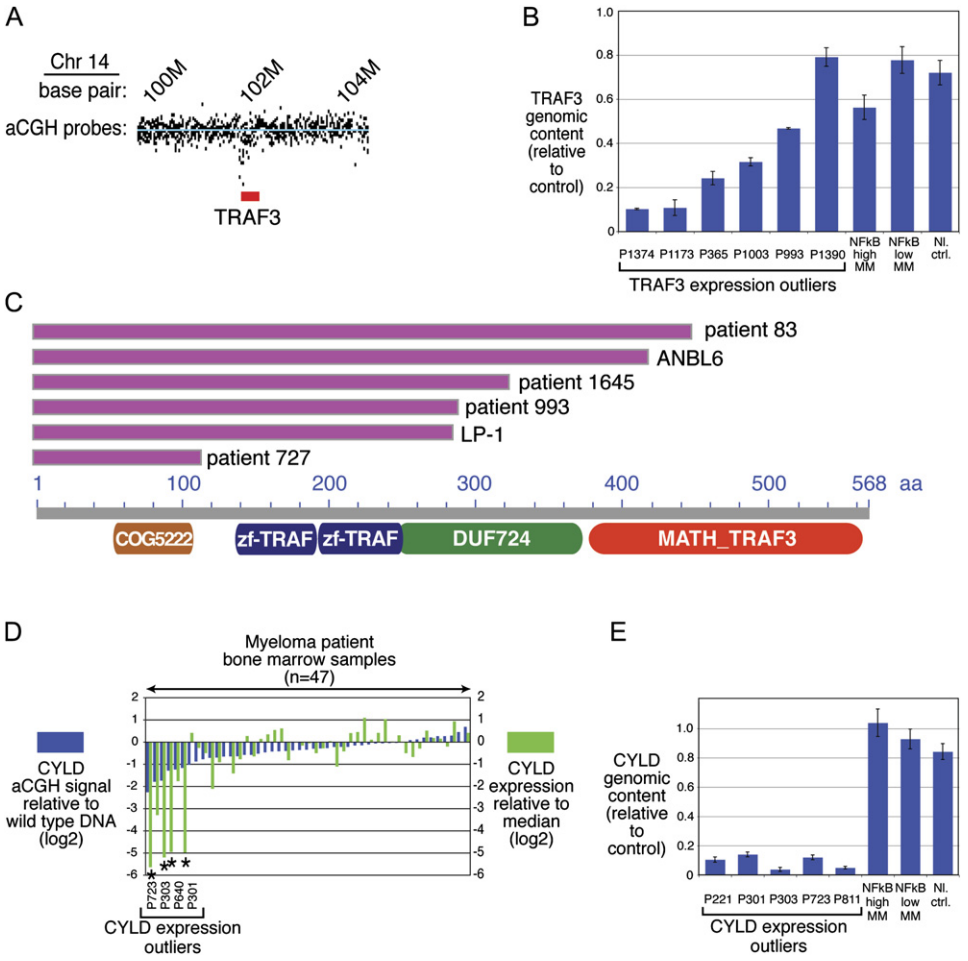

Figure 5. Genetic Abnormalities of the Negative NF-κB Regulators TRAF3 and CYLD in MM

(A) Genomic deletion of *TRAF3* in the OCI-MY1 cell line. aCGH estimated copy number from the *TRAF3* genomic region in OCI-MY1 versus a normal reference. Blue line indicates average ratio for probes within wild-type regions. The area depicted is ~3 Mb on chr 14 (NCBI build 35). Probes within the region encompassed by *TRAF3* (red) indicate genomic deletion of the *TRAF3* gene.

(B) qPCR analysis of *TRAF3* copy number. Copy number estimates of *TRAF3* relative to a control locus in six primary MM cases. Also shown is average copy number (±SE) in 12 cases, each with high or low NF-κB signature expression, and in ten normal control samples.

(C) Mutations in *TRAF3* that truncate the protein. Base pairs are numbered based on the *TRAF3* reference sequence NM_145725. Resequencing revealed nucleotide deletions or mutations in two NF-κB-positive MM cell lines (LP-1, ANBL-6) and in four patient samples. These changes produced early termination of the TRAF3 protein at the positions indicated in the diagram. Each mutation would delete all or part of the carboxy-terminal MATH domain required for binding to NIK and TNF receptor superfamily members.

(D) Comparison of aCGH and gene expression data for *CYLD* in MM samples. Cases are ranked according to their aCGH signals (Agilent probe 420863) relative to wild-type, with negative values indicating deletion, and compared with CYLD gene expression levels. The four *CYLD* gene expression outliers for which array CGH data were available are indicated.

(E) qPCR analysis of *CYLD* copy number. Copy number estimates of *CYLD* relative to a control locus in five primary MM cases. Also shown is average copy number (±SE) in 12 cases, each with high or low NF-κB signature expression, and in ten normal control samples.

OCI-My5 and KMM1 had high expression of *NFKB1*, with mRNA levels that were 4.5-fold and 18-fold higher expression than the median, respectively. aCGH revealed an ~25-fold amplification of the *NFKB1* gene in OCI-My5 (Figure S5A).

Two other cell lines, CAG and JK6L, had genetic abnormalities in *NFKB2*, encoding the p100 and p52 NF-κB subunits. Western blot revealed truncated forms of the NFKB2 protein (Figure S5B). JK6L had a homozygous frameshift mutation in *NFKB2*, disrupting the C-terminal ankyrin repeat domains, whereas CAG had a genomic deletion involving the *NFKB2* 3′ exons that truncated the mRNA and protein (Figures S5B–S5E). Such alterations were previously described in MM and other hematological malignancies and lead to nuclear forms of NFKB2 protein that are presumably constitutively active (Migliazza et al., 1994).

Examination of NF-κB target gene expression revealed that KMS18 and KMS28PE had exceedingly low expression of *BIRC3*, encoding the ubiquitin ligase cIAP2. These

two cell lines also had low expression of *BIRC2*, a gene that is next to *BIRC3* in the genome and encodes cIAP1, a ubiquitin ligase that inhibits TNFR signaling (Li et al., 2002). qPCR revealed that KMS18 and KMS28PE have homozygous deletions of the *BIRC2*/*BIRC3* chromosomal locus (Figure S5F). Six MM patient samples with low outlier expression of *BIRC3* and *BIRC2* (see above), and biallelic deletions in the *BIRC2*/*BIRC3* locus were detected by aCGH and/or qPCR (Figures S5F and S5G). All cell lines and patient samples with *BIRC2*/*BIRC3* deletions had NF-κB signature expression above the median (Figures 2F and 3B), suggesting that inactivation cIAP1 and/or cIAP2 may modulate the NF-κB pathway in MM.

NIK Protein Expression in MM Cell Lines

To explore the molecular mechanisms by which NIK overexpression activates the NF-κB pathway in MM, we first investigated the expression of NIK protein in cell lines. A high level of NIK protein was detected in five cell lines that were sensitive to IKKβ inhibition, including three with *NIK* genomic aberrations (EJM, JJN3, L363) but also two with no evidence of *NIK* aberrations (KMS28PE, KMS18) (Figure 6A). JJN3 cells had a 132 kD NIK protein instead of the 104 kD wild-type protein, which presumably is the EFTUD2-NIK fusion protein. A low level of NIK protein was detected in four other NF-κB-dependent cell lines (ANBL6, OCI-MY1, XG2, U266). Other NF-κB-dependent cell lines (OCI-My5, LP1, KMS28BM) lacked detectable NIK protein, as did all three NF-κB-negative cell lines (H929, JIM3, UTMC2).

The cell lines KMS18, KMS28PE, and JJN3 expressed *NIK* mRNA at an average level (Figure 6B), suggesting that these cell lines have translational or posttranslational mechanisms to elevate NIK protein levels. To investigate the latter possibility, we blocked protein synthesis with cycloheximide and monitored NIK protein abundance over time. The NIK protein in L363 cells was labile, with a half-life of less than 5 min, but the NIK proteins in KMS18, KMS28PE, and JJN3 were more stable, with half-lives greater than 30 min (Figure 6C). Treatment of L363 cells with the proteasome inhibitor bortezomib increased NIK protein levels dramatically, consistent with rapid protein turnover by ubiquitin-mediated proteolysis (Figure 6D). Proteosomal inhibition in KMS18 cells increased NIK protein levels to a much more modest extent (Figure 6D).

These data suggest that the high NIK protein levels in KMS18, KMS28PE, and JJN3 cells are achieved by post-translational stabilization of NIK protein. In JJN3, the EFTUD2-NIK fusion protein lacks amino acids 78–84 of NIK, required for TRAF3-mediated degradation of NIK, which could account for the stability of this protein. In KMS18 and KMS28PE, no alterations in the TRAF3-binding domain were present (data not shown). Intriguingly, both of these lines lack expression of *BIRC2* and *BIRC3* due to genomic deletions (Figure S5C), raising the possibility that cIAP1 and/or cIAP2 may play a role in NIK protein stability.

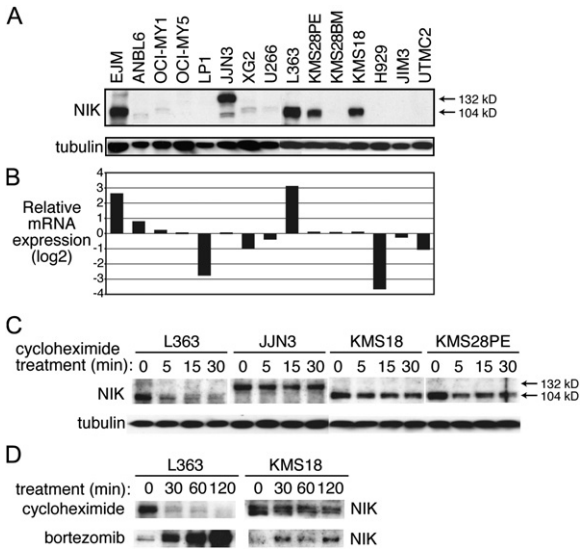

Figure 6. NIK Protein Overexpression in MM Cell Lines

(A) Western blot of NIK protein levels in cytoplasmic extracts from the indicated cell lines. The wild-type NIK protein is a 104 kD protein whereas the EFTUD2-NIK fusion protein in JJN3 is 132 kD.

(B) Relative *NIK* mRNA levels in cell lines as assessed by gene expression profiling on Affymetrix U133plus2.0 arrays (probe ID 205192_at).

(C) Enhanced NIK protein stability in a subset of myelomas. Western blot of NIK and tubulin levels before and after protein synthesis inhibition with cycloheximide.

(D) Proteasomal degradation of NIK varies in MM cell lines. L363 or KMS18 cells were treated with cycloheximide (20 μg/ml) or the proteasome inhibitor bortezomib (250 nM) for the indicated times and assayed for NIK levels.

NIK Overexpression Activates NF-κB Signaling and Blocks Cell Death in MM

To examine the functional significance of NIK overexpression in myeloma cell lines, we designed short hairpin RNAs (shRNAs) targeting *NIK* and expressed them in cell lines in an inducible fashion using retroviruses (Ngo et al., 2006). Two shRNAs against *NIK* were identified, one targeting the coding region and the other the 3′ untranslated region (UTR), which were capable of knocking down the wild-type *NIK* mRNA and protein expression (Figures 7A and 7B) as well as the EFTUD-NIK fusion protein in JJN3 (Figure 7F).

Induction of *NIK* shRNAs proved toxic to four cell lines with high NIK protein expression but not to four cell lines with low or absent NIK expression (Figure 7C). To demonstrate that *NIK* shRNA toxicity was due to knockdown of NIK protein, we performed a complementation experiment. EJM cells were engineered to express an exogenous *NIK* mRNA containing the coding region but lacking the 3′UTR. Expression of the 3′UTR-directed *NIK* shRNA in these cells was predicted to knock down the endogenous *NIK* mRNA but spare the exogenous *NIK* mRNA. Whereas the *NIK* shRNA was toxic for control EJM cells, cells expressing the exogenous *NIK* mRNA were rescued from this toxicity (Figure 7D). This experiment demonstrates that the *NIK* shRNA does not have appreciable off-target toxicity and supports the conclusion that NIK

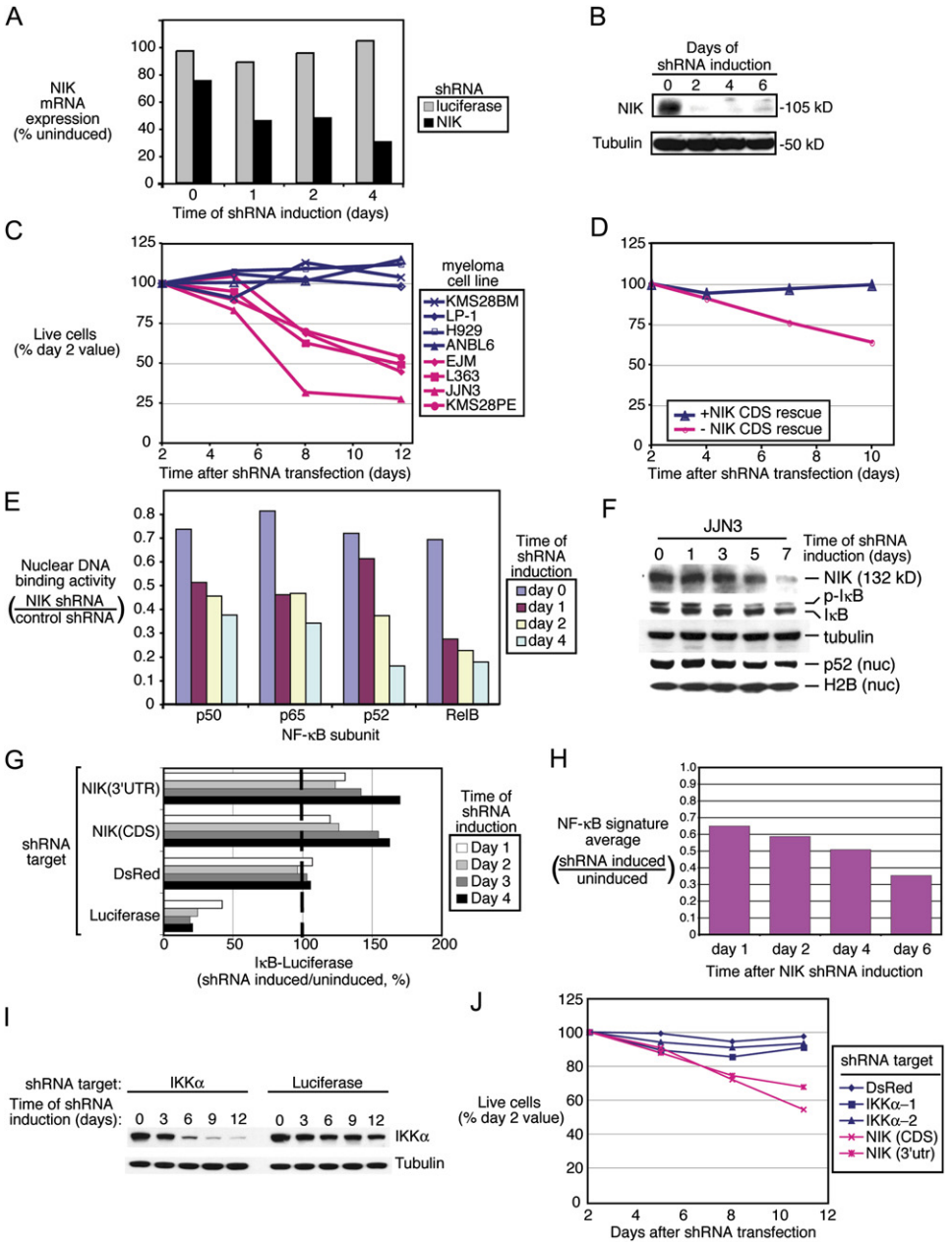

Figure 7. Knockdown of NIK Expression by RNA Interference Inhibits the NF-κB Pathway in MM

(A) Quantitative RT-PCR measurement of *NIK* mRNA levels following induction of the *NIK* shRNA in EJM cells.

(B) Western blot of NIK protein levels following induction of the *NIK* shRNA in EJM cells.

(C) Knockdown of NIK is toxic to NIK-overexpressing MM cell lines. The indicated cell lines were transduced with a retrovirus expressing the *NIK* shRNA (see Experimental Procedures). Live cells were enumerated by FACS and normalized to the value at day 2 following retroviral infection.

(D) Expression of the NIK coding sequence rescues cell lines transduced with an shRNA targeting the *NIK* 3′UTR. EJM cells expressing a NIK coding region cDNA or control EJM cells were transduced with a retrovirus expressing an shRNA targeting the *NIK* 3′UTR. Live cells were enumerated as in (C).

(E) Knockdown of NIK inhibits nuclear NF-κB DNA binding. DNA-binding activity by the indicated NF-κB subunits was quantified by ELISA.

(F) Knockdown of the EFTUD2-NIK fusion protein in JJN3 cells affects NF-κB signaling via classical and alternative pathways.

(G) Inhibition of IKK activity by knockdown of NIK in MM cell lines. EJM cells expressing an IκBα-luciferase fusion protein were superinfected with the indicated shRNAs. Induction of shRNAs targeting *NIK* caused a rise in luciferase activity indicating inhibition of IKK activity. Negative control shRNA targets DsRed; positive control shRNA targets luciferase.

(H) Inhibition of NF-κB target gene expression following knockdown of NIK in EJM cells. Relative expression of the NF-κB signature in shRNA induced versus uninduced cells is depicted.

(I) Western blot analysis of IKKα expression after induction of shRNAs targeting *IKKα* or luciferase. EJM cells were transduced with retroviral vectors expressing the indicated shRNAs, and expression of IKKα and tubulin was monitored at the indicated times.

expression is required for the survival of NIK-expressing cell lines.

We next investigated whether knockdown of NIK affected constitutive NF-κB signaling in MM cells. When *NIK* shRNA expression was induced, nuclear extracts had reduced DNA-binding activity of p50, p65, p52, and RelB, suggesting that NIK knockdown affected both the classical and alternative NF-κB pathways (Figure 7E). Likewise, knockdown of the EFTUD2-NIK fusion protein in JJN3 decreased phosphorylation of IκBα and abundance of nuclear p52, suggesting that this NIK protein also activates the classical and alternative pathways (Figure 7F).

The effect of NIK knockdown on IκBα kinase activity was measured in EJM cells engineered to express an IκBα-Photinus luciferase fusion protein, which increases in abundance when IKK activity is inhibited (Lam et al., 2005; Ngo et al., 2006). Induction of *NIK* shRNA increased luciferase activity, whereas an shRNA targeting DsRed had no effect and an shRNA targeting Photinus luciferase decreased the luciferase signal (Figure 7G). These data were consistent with the NF-κB DNA-binding assays and suggest that NIK functions upstream of IKKβ in this cell line. Accordingly, NF-κB target gene expression decreased in EJM cells during NIK knockdown (Figure 7H).

Since NIK can activate the alternative NF-κB pathway via IKKα, we tested whether IKKα depletion was toxic to the NIK-expressing cell line EJM. Two *IKKα* shRNAs strongly inhibited the expression of IKKα protein (Figure 7I). In contrast to the *NIK* shRNAs, these *IKKα* shRNAs were not toxic to EJM cells (Figure 7J) or other NIK-expressing cells (L363, JJN3, KMS28PE; data not shown), suggesting that the toxicity of *NIK* shRNAs was not due to blockade of the alternative NF-κB pathway.

TRAF3 Inactivation Promotes NF-κB Signaling and Cell Survival in MM

To investigate the influence of TRAF3 loss on NF-κB signaling in MM, we engineered two TRAF3-deficient cell lines, OCI-My1 and LP1, to express TRAF3 in a doxycycline-inducible fashion (Figure 8A). In both cell lines, TRAF3 induction was followed by a decrease in IκBα phosphorylation together with a decrease in total IκBα levels (Figure 8A). TRAF3 induction also led to a decrease in NF-κB signature expression (Figure 8B) and an increase in the IκBα-luciferase reporter (Figure 8C), indicative of IKK inhibition. DNA-binding activities of p50, p65, p52, and RelB in the nuclei of OCI-My1 cells were all decreased by TRAF3 induction (Figure 8D), suggesting that TRAF3 negatively regulates both the classical and alternative NF-κB pathways in these cells. Finally, induction of TRAF3 was toxic to both OCI-My1 and LP1, but not to H929, KMS28PE, and KMS28BM, which do not have TRAF3 abnormalities (Figure 8E). Together, these data suggest that TRAF3 inactivation in MM is likely to promote cell survival via NF-κB pathway activation.

DISCUSSION

The present study defined diverse molecular mechanisms activating NF-κB in MM. Most primary MM cases had high expression of the NF-κB signature. This observation suggests frequent engagement of the NF-κB pathway in myeloma for several reasons. First, the NF-κB signature genes were defined based on IKKβ inhibition and coexpression in myeloma cell lines, yet were nevertheless highly correlated in expression across primary patient samples. Second, the presence of the NF-κB p65 subunit in the nucleus of primary MM cells correlated with NF-κB signature expression. Finally, the genetic and epigenetic alterations that we defined were significantly skewed toward high NF-κB signature expression, in both MM patient samples ($p = 1.01 \times 10^{-9}$) and cell lines ($p = 1.08 \times 10^{-17}$) (Figures 2F, 3B, 3C, and 3G).

Some NF-κB pathway activation is likely related to signals that PCs receive in the bone marrow microenvironment. Indeed, among B cell subsets, normal PCs expressed the highest level of the NF-κB signature, presumably due to BAFF- and APRIL-mediated signaling (Hideshima et al., 2002; Marsters et al., 2000; Moreaux et al., 2005; O'Connor et al., 2004). Blockade of BAFF and APRIL decreases the number of bone marrow PCs in normal mice (O'Connor et al., 2004), raising the possibility that similar pharmacological inhibition might prove toxic to those MM cells that retain a microenvironmental dependence for NF-κB pathway activation.

However, the most compelling evidence for a critical role of the NF-κB pathway in myeloma pathogenesis was provided by the multiple, recurrent genetic abnormalities that we uncovered in the pathway. In cell lines and primary patient samples, NIK overexpression arose due to amplification or translocation of the *NIK* locus or due to enhanced NIK protein stability. An additional NF-κB-activating mechanism involved loss of functional TRAF3, either by homozygous deletion, inactivating mutations, or epigenetic silencing. Other genetic events associated with high NF-κB activity in MM included *CYLD* or *BIRC2*/*BIRC3* deletion, *CD40* overexpression, *NFKB1* amplification, and NFKB2 C-terminal truncation. Most of these genetic events increased classical and alternative NF-κB activity in MM cell lines, leading to pathway addiction and sensitivity to IKKβ inhibition. Taken together, these myriad genetic abnormalities strongly support the development of IKKβ inhibitors for the treatment of multiple myeloma.

NIK overexpression in MM cell lines activated both the classical and alternative NF-κB pathways. In normal mouse hematopoietic cells, loss of NIK does not affect activation of the classical pathway by inflammatory stimuli (Yin et al., 2001). However, NIK is required for the activation of the classical NF-κB pathway by certain TNF receptor family members, including CD40 (Ramakrishnan et al., 2004). Further, experimental overexpression of NIK can activate IKKβ and the classical pathway via

(J) Knockdown of IKKα is not toxic to a NIK-overexpressing myeloma. EJM cells were transduced with shRNAs targeting *IKKα*, *NIK*, or DsRed. Live cells were enumerated as in (C).

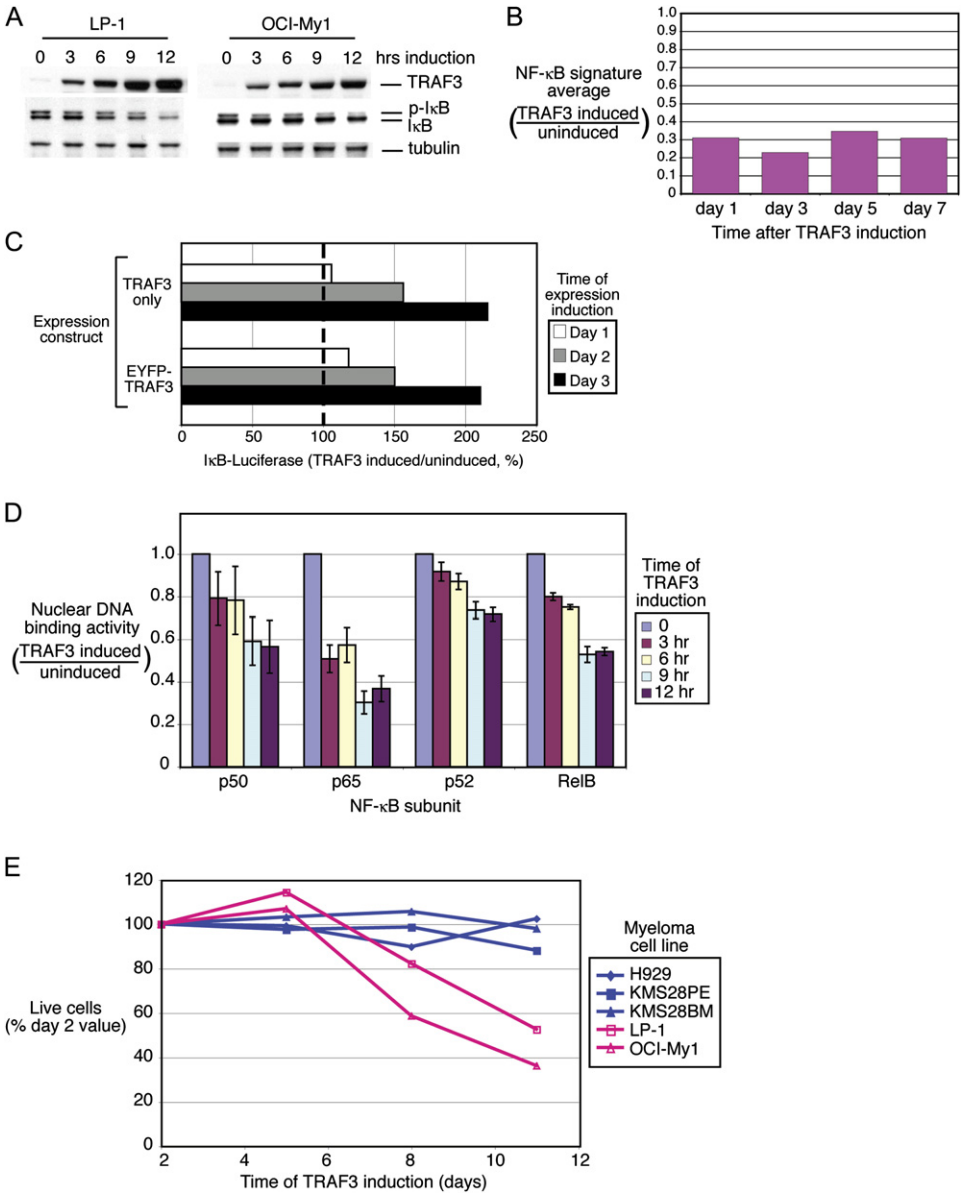

Figure 8. Effect of Re-Expression of TRAF3 in Cell Lines with TRAF3 Inactivation

(A) Inducible expression of TRAF3 in LP-1 and OCI-My1 cells decreases phosphorylated-IκBα (pIkB).

(B) Inhibition of NF-κB target gene expression following expression of TRAF3 in LP-1 cells. Relative expression of the NF-κB signature in TRAF3 induced versus uninduced cells is depicted.

(C) Inhibition of IKK activity by expression of TRAF3. OCI-My1 cells expressing an IκBα-luciferase fusion protein were superinfected with retroviruses expressing either wild-type TRAF3 or an EGFP-TRAF3 fusion protein. Induction of TRAF3 caused a rise in luciferase activity indicating inhibition of IKK activity.

(D) Effect of TRAF3 expression in OCI-My1 cells on the nuclear DNA-binding activity of the NF-κB p50, p65, p52, and RelB subunits. Binding to an oligonucleotide containing the NF-κB consensus sequence was measured in nuclear extracts prepared from cell lines induced to express TRAF3 relative to uninduced cells for the indicated times. DNA-binding activity was quantified by colorimetry (mean ± SD).

(E) Toxicity of TRAF3 expression in LP-1 and OCI-My1 cell lines with TRAF3 inactivation. The indicated myeloma cell lines were transduced with a retrovirus expressing TRAF3. Live cells were enumerated by FACS and normalized to the value at day 2 following retroviral infection.

phosphorylation of IKKβ in its activation loop (Delhase et al., 1999; O'Mahony et al., 2000). Indeed, NIK can form a complex with IKKα and IKKβ (Woronicz et al., 1997), perhaps by virtue of its ability to directly bind IKKα (Regnier et al., 1997). Studies conflict on the exact mechanism of IKKβ activation by NIK (Delhase et al., 1999; O'Mahony et al., 2000) but concur that NIK overexpression can activate IKKβ, supporting our finding that high NIK levels activate the classical NF-κB pathway in some myelomas.

We propose that the major mechanism by which NIK promotes tumor cell survival in MM is by stimulating IKKβ and activating the classical NF-κB pathway for several reasons. First, the toxicity of MLN for NIK-expressing MM cells argues for an essential role of IKKβ signaling: MLN is highly selective for IKKβ, with more than 1000-fold greater inhibitory activity for IKKβ than for 30 other cellular kinases, including IKKα (Nagashima et al., 2006). The IκBα super-repressor, which also specifically turns off the classical NF-κB pathway, resulted in similar toxicity and gene expression changes in these MM cells. Second, NIK depletion by shRNA inhibited IκBα kinase activity. Since IKKβ is a far more potent IκBα kinase than IKKα, this result suggests that NIK is activating IKKβ in these cells. Third, NIK knockdown decreased nuclear DNA-binding activity of the classical NF-κB subunits p50 and p65, consistent with an effect on IKKβ activity. Fourth, two shRNAs that effectively decreased IKKα protein expression were not toxic for NIK-expressing cell lines. These data support the argument that NIK acts through IKKβ to stimulate the classical NF-κB pathway, thereby promoting MM survival. Nonetheless, the alternative NF-κB pathway was also affected by NIK knockdown since p52 and RelB DNA-binding activity was reduced. It is therefore conceivable that activity of the alternative NF-κB pathway could contribute to the effect of NIK on cell survival.

Multiple mechanisms lead to high NIK protein expression in MM. The wild-type NIK protein had a very rapid turnover, and proteasome inhibition caused accumulation of NIK protein, consistent with a ubiquitin-mediated degradative pathway involving TRAF3, as described (Liao et al., 2004). Nevertheless, when wild-type *NIK* mRNA was expressed at extraordinarily high levels due to chromosomal aberrations, as in L363 and EJM cells, wild-type NIK protein accumulated. Cells with intermediate *NIK* mRNA levels engage various mechanisms to stabilize NIK protein. In JJN3 cells, a chromosomal translocation precisely removed the region of NIK that TRAF3 requires to destabilize NIK protein (Liao et al., 2004), highlighting the interrelationship of TRAF3 and NIK in MM pathogenesis. KMS28PE and KMS18 had enhanced stability of NIK protein without evident alterations in the TRAF3-binding domain of NIK or in TRAF3 itself. Both KMS18 and KMS28PE had genomic deletions of the *BIRC2/BIRC3* genomic locus, which encodes the ubiquitin ligases cIAP1 and cIAP2. cIAP1 attenuates NF-κB signaling from TNFR2 (Li et al., 2002), raising the possibility that this protein or cIAP2 may also inhibit NF-κB signaling downstream of NIK by decreasing NIK protein stability.

Another recurrent mechanism of NF-κB activation in myeloma was silencing, homozygous deletion, or somatic mutation of *TRAF3*. In primary MM patient samples, 4.4% had a *TRAF3* abnormality, and these cases had higher NF-κB signature expression than other myelomas. Homozygous *TRAF3* deletions occurred in two primary cases and in the OCI-My1 cell line. In addition, two NF-κB-dependent cell lines and four primary patient samples carried homozygous mutations creating truncated TRAF3 proteins that should be incapable of interacting with NIK or TNFR superfamily members. In cases lacking deletion or mutation of *TRAF3*, low *TRAF3* mRNA expression may be due to epigenetic silencing, a frequent event in cancer.

Experimental re-expression of TRAF3 in cell lines lacking functional TRAF3 decreased IKKβ activity and both classical and alternative NF-κB signaling, resulting in cell death. The precise mechanism by which TRAF3 modulates IKK activity in these cell lines remains to be elucidated. The cell lines with inactive TRAF3 do not have high NIK protein expression. Moreover, one of the TRAF3 mutant cells, LP1, was not affected by the *NIK* shRNA. In this cell line, therefore, TRAF3 must affect IKKβ activity by a NIK-independent mechanism.

In primary MM, the full consequence of TRAF3 inactivation may only be evident in cells dependent on NF-κB signaling from a TNFR family member that can be negatively regulated by TRAF3 (Hauer et al., 2005). The most logical candidate cytokines to propagate TRAF3-deficient MM are BAFF and APRIL, which are abundant in the bone marrow and can signal through TACI and BCMA, two TNFRs that are highly expressed in a subset of MM (Moreaux et al., 2005).

It is also notable that extreme overexpression of *CD40*, a TNFR family member, was associated with NF-κB activation in MM. CD40 and other members of the TNFR superfamily can activate NF-κB when overexpressed, even in the absence of ligand (Lee et al., 1996; Rothe et al., 1995b; Yamamoto et al., 1998). It is therefore plausible that the 34-fold average overexpression of *CD40* in the *CD40* outlier cases is sufficient to activate NF-κB in a cell-autonomous fashion.

A key negative regulator of NF-κB signaling is CYLD, which was homozygously deleted in primary MM cases with high NF-κB signature expression. CYLD is a deubiquitinating enzyme that removes ubiquitin moieties from activated TRAF2, TRAF6, IKKγ, and BCL3, thereby interfering with NF-κB signaling at multiple regulatory levels (Brummelkamp et al., 2003; Kovalenko et al., 2003; Massoumi et al., 2006; Regamey et al., 2003; Trompouki et al., 2003). Of note, CYLD was ineffective in inhibiting NF-κB activity induced by NIK overexpression (Kovalenko et al., 2003).

It therefore appears that diverse upstream signaling pathways activate IKKβ in MM. Further, some myelomas may bypass the requirement for IKK altogether by amplifying and overexpressing *NFKB1*, encoding the p50 subunit of the classical NF-κB pathway, or by creating truncated and constitutively active NFKB2 proteins. The recurrent yet varied nature of these genetic abnormalities suggests strongly that activity of the NF-κB pathway is the phenotype that is selected rather than any particular genetic lesion.

Overall, we documented genetic abnormalities in the NF-κB pathway in 13 (28%) MM cell lines and 41 (9%) of the primary MM samples. Considering that we resequenced *TRAF3* in only 10% of the patient samples, a larger number of *TRAF3* mutations probably exist within our sample set. Therefore, the total number of genetic

abnormalities in the genes we studied can be predicted to be ~16%. Given the large number and variety of genetic abnormalities discovered in the present report, there may well be genetic aberrations in other components of the NF-κB pathway that we have not studied. As already mentioned, however, many MM cases with high NF-κB signature expression may not have genetic abnormalities in the NF-κB pathway but rather may derive activating signals from the microenvironment. Irrespective of whether the activation of the NF-κB pathway is cell intrinsic or cell extrinsic, the MM cell may nonetheless depend upon this pathway for survival.

A clear message from these recurrent yet varied genetic abnormalities is that the NF-κB pathway plays a pervasive role in the pathogenesis of MM, providing a strong impetus to the development of NF-κB pathway inhibitors for the therapy of this malignancy. Currently, IKKβ inhibitors are under development for clinical use and are likely to have manageable on-target side effects (Nagashima et al., 2006). That the majority of MM cell lines tested retained a dependence on NF-κB signaling for survival is encouraging and consistent with previous results (Hideshima et al., 2006). The NF-κB signature provides a basis to develop biomarkers of response to NF-κB pathway inhibitors. A gauge of NF-κB activity, such as quantitative RT-PCR to measure the 11-gene NF-κB signature, could be assessed in bone marrow MM samples both pretreatment and during administration of the drug. Coupling biomarkers with pathway-targeted therapeutics will ultimately allow treatment of MM patients to be tailored to the genetic abnormalities of their cancers.

EXPERIMENTAL PROCEDURES

Primary MM Patient Samples

Primary MM cells were purified from bone marrow aspirates obtained under approval of the Institutional Review Board of the University of Arkansas for Medical Sciences (Little Rock, AR). Written informed consent was documented. MM plasma cells were isolated by CD138 immunomagnetic bead selection (Zhan et al., 2006).

Cell Culture, Retroviral Constructs, and Transduction

MM cell lines were maintained in RPMI 1640 or ACL-4 medium supplemented with 10% fetal calf serum (Hyclone) and penicillin/streptomycin (Invitrogen) with or without 10 ng/ml IL-6 (R&D Systems). The IKKβ inhibitor MLN120b was provided by Millennium Pharmaceuticals (Cambridge, MA). For efficient retroviral transductions, cell lines were engineered to express the murine ecotropic retroviral receptor (Lam et al., 2005). Certain cell lines were also engineered to express the bacterial tetracycline repressor (TETR) (Ngo et al., 2006). All inducible constructs in TETR lines were activated by doxycycline (20 ng/ml).

To assess toxicity of an shRNA, retroviruses that coexpressed GFP were used as described (Ngo et al., 2006). In brief, flow cytometry was performed 2 days after retroviral infection to determine the initial GFP-positive proportion of live cells for each shRNA, then cells were subsequently cultured with doxycycline to induce shRNA and sampled over time. The GFP-positive proportion at each time was normalized to that for the control shRNA (against luciferase), and further normalized to the initial value.

The cell-based assay for IKK activity was performed as described (Ngo et al., 2006) using a TETR cell line engineered to express Renilla luciferase and a fusion protein of IκBα and firefly luciferase (IκBα-Photinus); after infection with shRNA vectors and puromycin selection, shRNA was induced and samples were measured for the two reporters using the Dual-Glo luciferase assay system (Promega).

FISH

Three-color FISH assays of metaphase chromosomes derived from MM cell lines were performed as described (Shou et al., 2000). In addition to the previously described immunoglobulin probes, a 92 kb PAC (AC003963, version gi:2978476) was used as a probe for *NIK*. Using the same probes, *NIK* copy number alterations and *NIK-IGH* and *NIK-IGL* gene fusions were evaluated by triple color interphase FISH on mononuclear cells from bone marrow aspirates of newly diagnosed disease (Hanamura et al., 2006).

Polymorphism to Distinguish NIK Alleles

A CT polymorphism at base pair 3020 (reference mRNA NM_003954) in the 3′ untranslated region of *NIK* RNA was identified from the human EST database. Sequence analysis of PCR products from genomic DNA was determined for 16 MM cell lines and 14 primary MM tumors. Nine samples each had only C or T alleles, and 12 samples had both C and T. When both alleles were present, the assay was repeated using cDNA to distinguish mono- versus biallelic expression.

Cloning of Translocation Breakpoints

Southern blotting was used to identify rearranged HpaI genomic fragments within or near the *NIK* gene for the L363 and JJN3 cell lines. Genomic libraries were made from HpaI fragments modified with BamHI adaptors that were cloned in the λDash II vector (Stratagene) and then screened with the probes used for the Southern blots. The sequence of inserts was obtained directly (L363) or from a PCR product (JJN3).

Western Blot and ELISA

Protein was harvested from MM cell lines and fractionated using a Nuclear/cytosol fractionation kit (BioVision). Protein was quantified using the BCA method (Pierce) and separated by SDS-PAGE on a 4%–12% acrylamide gradient. Nuclear protein was analyzed for NF-κB activity using the TransAm NF-κB family kit (Active Motif). The following antibodies were used: NIK, phospho-IκBα (Cell signaling), IκBα, p65 (SantaCruz Biotechnologies), p52/p100 (Upstate), B-tubulin (Sigma), histone H2B (Imgenex).

qPCR

Copy number of *TRAF3*, *BIRC2*, *BIRC3*, and *CYLD* was measured in DNA extracted from CD138+ MM samples or mononuclear cells purified from peripheral blood of normal donors. qPCR was performed and normalized to the *PRKCQ* locus as described (Rosenwald et al., 2003). Primer sequences are listed in the Supplemental Experimental Procedures.

aCGH

DNA from MM cell lines was labeled fluorescently with Cy5, and normal control genomic DNA was labeled with Cy3. These probes were cohybridized to 400,000 element Nimblegen whole-genome arrays. Intensity of hybridized probes was determined using an Axon scanner, and data were analyzed with Nimblegen Scanarray software. Previous aCGH data on 47 MM samples were downloaded for comparison with gene expression (Carrasco et al., 2006).

Gene Expression Profiling and Analysis

Lymphochip DNA microarrays were utilized as described (Alizadeh et al., 2000). Normal human B cell subsets were purified as described (Alizadeh et al., 2000; Nilsson et al., 2000) and profiled following linear mRNA amplification (see Supplemental Experimental Procedures for details). Microarray data from primary MM samples were obtained from http://www.ncbi.nlm.nih.gov/geo/ (accession number GSE2658) (Shaughnessy et al., 2007; Zhan et al., 2006).

Genes comprising the NF-κB signature in MM were those that were decreased in expression by >40% in at least six of eight time points following treatment of L363 cells with MLN for 8–24 hr in three separate

experiments (accession number GSE8487). Genes were chosen if they correlated in expression across the MM cell lines ($r > 0.5$). See the Supplemental Data for Affymetrix U133plus2.0 probe sets used for analysis.

Analysis of outlier gene expression was performed as described (Tomlins et al., 2005). Briefly, data from each Affymetrix probe set were median centered across all samples. The absolute difference from the median was calculated for each sample, and the data were scaled such that the median of these values was 1 (log2). Outlier gene expression was defined to be any scaled values greater than 5 (log2). In other words, compared to the median deviation of samples from the median, outlier cases had >32-fold larger deviation. For a set of cases with outlier expression of a particular gene, the association of this outlier profile with the NF-κB signature was calculated by comparing expression of the NF-κB signature in outliers versus other cases using a Student's t test. To adjust for the influence of gene expression differences among known MM subgroups (Zhan et al., 2006), we fitted an analysis of variance model for log signal of the NF-κB signature, including MM subgroup as a categorical variable and outlier status as a two-categorical variable.

The p value describes the association of NF-κB pathway abnormalities with high NF-κB signature expression, based on a Wilcoxon signed rank test.

See the Supplemental Data for additional Experimental Procedures.

Supplemental Data

The Supplemental Data include Supplemental Experimental Procedures, five supplemental figures, and array CGH data from OCI-My1 and OCI-My5 cell lines and can be found with this article online at http://www.cancercell.org/cgi/content/full/12/2/115/DC1/.

ACKNOWLEDGMENTS

This research was supported by the Intramural Research Program of the NIH, National Cancer Institute, Center for Cancer Research (L.M.S., W.M.K.); NIH grant CA55819 (B.B. and J.D.S.); and the Lebow Fund for the Cure (J.D.S.). L.D. is an employee of Millennium Pharmaceuticals, Inc., Cambridge, MA. The authors would like to acknowledge the technical contributions of Leslie Brents. W.M.K. thanks Leif Bergsagel for suggesting the possibility of a NIK translocation in JJN3 cells.

Received: December 14, 2006
Revised: May 4, 2007
Accepted: July 18, 2007
Published: August 13, 2007

REFERENCES

Alizadeh, A.A., Eisen, M.B., Davis, R.E., Ma, C., Lossos, I.S., Rosenwald, A., Boldrick, J.C., Sabet, H., Tran, T., Yu, X., et al. (2000). Distinct types of diffuse large B-cell lymphoma identified by gene expression profiling. Nature *403*, 503–511.

Barlogie, B., Shaughnessy, J., Tricot, G., Jacobson, J., Zangari, M., Anaissie, E., Walker, R., and Crowley, J. (2004). Treatment of multiple myeloma. Blood *103*, 20–32.

Basseres, D.S., and Baldwin, A.S. (2006). Nuclear factor-κB and inhibitor of κB kinase pathways in oncogenic initiation and progression. Oncogene *25*, 6817–6830.

Berberich, I., Shu, G.L., and Clark, E.A. (1994). Cross-linking CD40 on B cells rapidly activates nuclear factor-κB. J. Immunol. *153*, 4357–4366.

Brummelkamp, T.R., Nijman, S.M., Dirac, A.M., and Bernards, R. (2003). Loss of the cylindromatosis tumour suppressor inhibits apoptosis by activating NF-κB. Nature *424*, 797–801.

Carrasco, D.R., Tonon, G., Huang, Y., Zhang, Y., Sinha, R., Feng, B., Stewart, J.P., Zhan, F., Khatry, D., Protopopova, M., et al. (2006). High-resolution genomic profiles define distinct clinico-pathogenetic subgroups of multiple myeloma patients. Cancer Cell *9*, 313–325.

Claudio, E., Brown, K., Park, S., Wang, H., and Siebenlist, U. (2002). BAFF-induced NEMO-independent processing of NF-κB2 in maturing B cells. Nat. Immunol. *3*, 958–965.

Coope, H.J., Atkinson, P.G., Huhse, B., Belich, M., Janzen, J., Holman, M.J., Klaus, G.G., Johnston, L.H., and Ley, S.C. (2002). CD40 regulates the processing of NF-κB2 p100 to p52. EMBO J. *21*, 5375–5385.

Davis, R.E., Brown, K.D., Siebenlist, U., and Staudt, L.M. (2001). Constitutive nuclear factor κB activity is required for survival of activated B cell-like diffuse large B cell lymphoma cells. J. Exp. Med. *194*, 1861–1874.

Delhase, M., Hayakawa, M., Chen, Y., and Karin, M. (1999). Positive and negative regulation of IκB kinase activity through IKKβ subunit phosphorylation. Science *284*, 309–313.

Ghosh, S., and Karin, M. (2002). Missing pieces in the NF-κB puzzle. Cell *Suppl*. *109*, S81–S96.

Hanamura, I., Stewart, J.P., Huang, Y., Zhan, F., Santra, M., Sawyer, J.R., Hollmig, K., Zangarri, M., Pineda-Roman, M., van Rhee, F., et al. (2006). Frequent gain of chromosome band 1q21 in plasma-cell dyscrasias detected by fluorescence in situ hybridization: Incidence increases from MGUS to relapsed myeloma and is related to prognosis and disease progression following tandem stem-cell transplantation. Blood *108*, 1724–1732.

Hauer, J., Puschner, S., Ramakrishnan, P., Simon, U., Bongers, M., Federle, C., and Engelmann, H. (2005). TNF receptor (TNFR)-associated factor (TRAF) 3 serves as an inhibitor of TRAF2/5-mediated activation of the noncanonical NF-κB pathway by TRAF-binding TNFRs. Proc. Natl. Acad. Sci. USA *102*, 2874–2879.

Hideshima, T., Chauhan, D., Richardson, P., Mitsiades, C., Mitsiades, N., Hayashi, T., Munshi, N., Dang, L., Castro, A., Palombella, V., et al. (2002). NF-κB as a therapeutic target in multiple myeloma. J. Biol. Chem. *277*, 16639–16647.

Hideshima, T., Neri, P., Tassone, P., Yasui, H., Ishitsuka, K., Raje, N., Chauhan, D., Podar, K., Mitsiades, C., Dang, L., et al. (2006). MLN120B, a novel IκB kinase β inhibitor, blocks multiple myeloma cell growth in vitro and in vivo. Clin. Cancer Res. *12*, 5887–5894.

Jemal, A., Siegel, R., Ward, E., Murray, T., Xu, J., Smigal, C., and Thun, M.J. (2006). Cancer statistics, 2006. CA Cancer J. Clin. *56*, 106–130.

Kovalenko, A., Chable-Bessia, C., Cantarella, G., Israel, A., Wallach, D., and Courtois, G. (2003). The tumour suppressor CYLD negatively regulates NF-κB signalling by deubiquitination. Nature *424*, 801–805.

Lam, L.T., Davis, R.E., Pierce, J., Hepperle, M., Xu, Y., Hottelet, M., Nong, Y., Wen, D., Adams, J., Dang, L., and Staudt, L.M. (2005). Small molecule inhibitors of IkB-kinase are selectively toxic for subgroups of diffuse large B cell lymphoma defined by gene expression profiling. Clin. Cancer Res. *11*, 28–40.

Lee, S.Y., Kandala, G., Liou, M.L., Liou, H.C., and Choi, Y. (1996). CD30/TNF receptor-associated factor interaction: NF-κB activation and binding specificity. Proc. Natl. Acad. Sci. USA *93*, 9699–9703.

Li, X., Yang, Y., and Ashwell, J.D. (2002). TNF-RII and c-IAP1 mediate ubiquitination and degradation of TRAF2. Nature *416*, 345–347.

Li, C., Norris, P.S., Ni, C.Z., Havert, M.L., Chiong, E.M., Tran, B.R., Cabezas, E., Reed, J.C., Satterthwait, A.C., Ware, C.F., and Ely, K.R. (2003). Structurally distinct recognition motifs in lymphotoxin-β receptor and CD40 for tumor necrosis factor receptor-associated factor (TRAF)-mediated signaling. J. Biol. Chem. *278*, 50523–50529.

Liao, G., Zhang, M., Harhaj, E.W., and Sun, S.C. (2004). Regulation of the NF-κB-inducing kinase by tumor necrosis factor receptor-associated factor 3-induced degradation. J. Biol. Chem. *279*, 26243–26250.

Marsters, S.A., Yan, M., Pitti, R.M., Haas, P.E., Dixit, V.M., and Ashkenazi, A. (2000). Interaction of the TNF homologues BLyS and APRIL with the TNF receptor homologues BCMA and TACI. Curr. Biol. *10*, 785–788.

Massoumi, R., Chmielarska, K., Hennecke, K., Pfeifer, A., and Fassler, R. (2006). Cyld inhibits tumor cell proliferation by blocking Bcl-3-dependent NF-κB signaling. Cell *125*, 665–677.

Migliazza, A., Lombardi, L., Rocchi, M., Trecca, D., Chang, C.C., Antonacci, R., Fracchiolla, N.S., Ciana, P., Maiolo, A.T., and Neri, A. (1994). Heterogeneous chromosomal aberrations generate 3′ truncations of the NFKB2/lyt-10 gene in lymphoid malignancies. Blood *84*, 3850–3860.

Mitsiades, C.S., Mitsiades, N., Munshi, N.C., and Anderson, K.C. (2004). Focus on multiple myeloma. Cancer Cell *6*, 439–444.

Moreaux, J., Cremer, F.W., Reme, T., Raab, M., Mahtouk, K., Kaukel, P., Pantesco, V., De Vos, J., Jourdan, E., Jauch, A., et al. (2005). The level of TACI gene expression in myeloma cells is associated with a signature of microenvironment dependence versus a plasmablastic signature. Blood *106*, 1021–1030.

Nagashima, K., Sasseville, V.G., Wen, D., Bielecki, A., Yang, H., Simpson, C., Grant, E., Hepperle, M., Harriman, G., Jaffee, B., et al. (2006). Rapid TNFR1-dependent lymphocyte depletion in vivo with a selective chemical inhibitor of IKKβ. Blood *107*, 4266–4273.

Ngo, V.N., Davis, R.E., Lamy, L., Yu, X., Zhao, H., Lenz, G., Lam, L.T., Dave, S., Yang, L., Powell, J., and Staudt, L.M. (2006). A loss-of-function RNA interference screen for molecular targets in cancer. Nature *441*, 106–110.

Ni, C.Z., Welsh, K., Leo, E., Chiou, C.K., Wu, H., Reed, J.C., and Ely, K.R. (2000). Molecular basis for CD40 signaling mediated by TRAF3. Proc. Natl. Acad. Sci. USA *97*, 10395–10399.

Ni, C.Z., Oganesyan, G., Welsh, K., Zhu, X., Reed, J.C., Satterthwait, A.C., Cheng, G., and Ely, K.R. (2004). Key molecular contacts promote recognition of the BAFF receptor by TNF receptor-associated factor 3: Implications for intracellular signaling regulation. J. Immunol. *173*, 7394–7400.

Nilsson, N., Ingvarsson, S., and Borrebaeck, C.A. (2000). Immature B cells in bone marrow express Fas/FasL. Scand. J. Immunol. *51*, 279–284.

O'Connor, B.P., Raman, V.S., Erickson, L.D., Cook, W.J., Weaver, L.K., Ahonen, C., Lin, L.L., Mantchev, G.T., Bram, R.J., and Noelle, R.J. (2004). BCMA is essential for the survival of long-lived bone marrow plasma cells. J. Exp. Med. *199*, 91–98.

O'Mahony, A., Lin, X., Geleziunas, R., and Greene, W.C. (2000). Activation of the heterodimeric IκB kinase α (IKKα)-IKKβ complex is directional: IKKα regulates IKKβ under both basal and stimulated conditions. Mol. Cell. Biol. *20*, 1170–1178.

Qing, G., Qu, Z., and Xiao, G. (2005). Stabilization of basally translated NF-κB-inducing kinase (NIK) protein functions as a molecular switch of processing of NF-κB2 p100. J. Biol. Chem. *280*, 40578–40582.

Ramakrishnan, P., Wang, W., and Wallach, D. (2004). Receptor-specific signaling for both the alternative and the canonical NF-κB activation pathways by NF-κB-inducing kinase. Immunity *21*, 477–489.

Regamey, A., Hohl, D., Liu, J.W., Roger, T., Kogerman, P., Toftgard, R., and Huber, M. (2003). The tumor suppressor CYLD interacts with TRIP and regulates negatively nuclear factor κB activation by tumor necrosis factor. J. Exp. Med. *198*, 1959–1964.

Regnier, C.H., Song, H.Y., Gao, X., Goeddel, D.V., Cao, Z., and Rothe, M. (1997). Identification and characterization of an IκB kinase. Cell *90*, 373–383.

Rosenwald, A., Wright, G., Leroy, K., Yu, X., Gaulard, P., Gascoyne, R.D., Chan, W.C., Zhao, T., Haioun, C., Greiner, T.C., et al. (2003). Molecular diagnosis of primary mediastinal B cell lymphoma identifies a clinically favorable subgroup of diffuse large B cell lymphoma related to Hodgkin lymphoma. J. Exp. Med. *198*, 851–862.

Rothe, M., Pan, M.G., Henzel, W.J., Ayres, T.M., and Goeddel, D.V. (1995a). The TNFR2-TRAF signaling complex contains two novel proteins related to baculoviral inhibitor of apoptosis proteins. Cell *83*, 1243–1252.

Rothe, M., Sarma, V., Dixit, V.M., and Goeddel, D.V. (1995b). TRAF2-mediated activation of NF-κB by TNF receptor 2 and CD40. Science *269*, 1424–1427.

Senftleben, U., Cao, Y., Xiao, G., Greten, F.R., Krahn, G., Bonizzi, G., Chen, Y., Hu, Y., Fong, A., Sun, S.C., and Karin, M. (2001). Activation by IKKα of a second, evolutionary conserved, NF-κB signaling pathway. Science *293*, 1495–1499.

Shaughnessy, J.D., Jr., Zhan, F., Burington, B.E., Huang, Y., Colla, S., Hanamura, I., Stewart, J.P., Kordsmeier, B., Randolph, C., Williams, D.R., et al. (2007). A validated gene expression model of high-risk multiple myeloma is defined by deregulated expression of genes mapping to chromosome 1. Blood *109*, 2276–2284. Published online November 14, 2006. 10.1182/blood-2006-07-038430.

Shou, Y., Martelli, M.L., Gabrea, A., Qi, Y., Brents, L.A., Roschke, A., Dewald, G., Kirsch, I.R., Bergsagel, P.L., and Kuehl, W.M. (2000). Diverse karyotypic abnormalities of the c-myc locus associated with c-myc dysregulation and tumor progression in multiple myeloma. Proc. Natl. Acad. Sci. USA *97*, 228–233.

Tomlins, S.A., Rhodes, D.R., Perner, S., Dhanasekaran, S.M., Mehra, R., Sun, X.W., Varambally, S., Cao, X., Tchinda, J., Kuefer, R., et al. (2005). Recurrent fusion of TMPRSS2 and ETS transcription factor genes in prostate cancer. Science *310*, 644–648.

Trompouki, E., Hatzivassiliou, E., Tsichritzis, T., Farmer, H., Ashworth, A., and Mosialos, G. (2003). CYLD is a deubiquitinating enzyme that negatively regulates NF-κB activation by TNFR family members. Nature *424*, 793–796.

Woronicz, J.D., Gao, X., Cao, Z., Rothe, M., and Goeddel, D.V. (1997). IκB kinase-β: NF-κB activation and complex formation with IκB kinase-α and NIK. Science *278*, 866–869.

Xiao, G., and Sun, S.C. (2000). Negative regulation of the nuclear factor κB-inducing kinase by a cis-acting domain. J. Biol. Chem. *275*, 21081–21085.

Xiao, G., Harhaj, E.W., and Sun, S.C. (2001). NF-κB-inducing kinase regulates the processing of NF-κB2 p100. Mol. Cell *7*, 401–409.

Yamamoto, H., Kishimoto, T., and Minamoto, S. (1998). NF-κB activation in CD27 signaling: Involvement of TNF receptor-associated factors in its signaling and identification of functional region of CD27. J. Immunol. *161*, 4753–4759.

Yin, L., Wu, L., Wesche, H., Arthur, C.D., White, J.M., Goeddel, D.V., and Schreiber, R.D. (2001). Defective lymphotoxin-β receptor-induced NF-κB transcriptional activity in NIK-deficient mice. Science *291*, 2162–2165.

Zhan, F., Hardin, J., Kordsmeier, B., Bumm, K., Zheng, M., Tian, E., Sanderson, R., Yang, Y., Wilson, C., Zangari, M., et al. (2002). Global gene expression profiling of multiple myeloma, monoclonal gammopathy of undetermined significance, and normal bone marrow plasma cells. Blood *99*, 1745–1757.

Zhan, F., Huang, Y., Colla, S., Stewart, J.P., Hanamura, I., Gupta, S., Epstein, J., Yaccoby, S., Sawyer, J., Burington, B., et al. (2006). The molecular classification of multiple myeloma. Blood *108*, 2020–2028.

Zhan, F., Barlogie, B., Arzoumanian, V., Huang, Y., Williams, D.R., Hollmig, K., Pineda-Roman, M., Tricot, G., van Rhee, F., Zangari, M., et al. (2007). Gene-expression signature of benign monoclonal gammopathy evident in multiple myeloma is linked to good prognosis. Blood *109*, 1692–1700.

Accession Numbers

The gene expression profiling data from cell line L363 treated with the IKKβ inhibitor and EJM with the inducible IκBα super-repressor have been deposited in the Gene Expression Omnibus (GEO accession number GSE8487).